

## SUPPORTING ONLINE MATERIAL

### Materials and Methods

ES cell targeting. The SLK2 backbone for the Mx-Lox vector contains the puromycin resistance gene (pPUR, Clontech, Palo Alto, CA) under the PGK promoter (1), and a LoxP site and 5' neomycin resistance gene (pBS226, Gibco) under the Pol II promoter (2), cloned into Bam HI and Eco RV sites of RS313 (3). The diphtheria toxin A gene (4) was cloned into the Xho I site of RS313. The short arm of genomic sequence from the *Mx* region was a 2.3 kb Eco RV / Hind III restriction fragment, cloned from PAC RPCI-21\_454K24 (5) into corresponding sites in pBluescript (Stratagene, La Jolla, CA). This arm was shortened to 0.9 kb by digestion at an internal Bam HI site, which was blunted, released from pBluescript with Not I digestion, and cloned into SLK2 at Nae I and Not I sites. The long arm of genomic sequence was a 6.2 kb Eco RI / Taq I restriction fragment, cloned from the same PAC into Eco RI and Cla I sites in pBluescript. This arm was isolated from the pBluescript Xho I and Sma I polylinker sites, and cloned into the SLK2 vector at Xho I and blunted Cla I sites.

MC1 embryonic stem cells were derived from 129S6/SvEv mice at the Johns Hopkins University Transgenic Core Facility and were cultured in 15% serum at 37 °C and 5% CO<sub>2</sub> on mitomycin-treated embryonic fibroblast feeder cells. Mx-Lox targeting vector (25 µg) was linearized with Fsp I and electroporated into 1 x 10<sup>7</sup> MC1 cells or cells which were previously targeted at *Cbr1* (6) at 0.32 kV and 250 µF using a BioRad (Hercules, CA) electroporator, and colonies were selected in 1.0 µg/ml puromycin (Sigma, St. Louis, MO). Puromycin resistant cell lines were screened with PCR primers MXF1 (5' CCAGTGTTCTGCTTAGGT 3') and SLK2R1 (5' CCCCTGAACCTGAAACAT 3'). PCR reactions contained 2 mM MgCl<sub>2</sub> and were performed for 30 cycles of denaturation (15 s 94 °C), annealing (1 min 55 °C), and extension (1:30 min 72 °C). Targeting was confirmed with genomic DNA Southern blot analysis using random primed <sup>32</sup>P-labeled probes amplified with PCR primers MXF2 (5' GGGCTTATTTCTCTTCAGCT 3') and MXR2 (5' GATGCAAGGCCACTAGAA 3'), and MXF3 (5' CTTGCTTGAACCAGGCCTA 3') and MXR3 (5' CACAGCCACAGGAAGGTA 3').

CAGGS-Cre vector (6.25 µg)(7) was electroporated under the above conditions into 2.5 x 10<sup>6</sup> cells of each double LoxP-targeted line and G418 (Invitrogen, Carlsbad, CA) selection was added 48 hours after transfection at 250 µg/ml. Twelve to fifteen cells with the deleted and duplicated DSCR chromosomes were injected into each of approximately one hundred ICR blastocysts and transferred to ten surrogate mothers. Typing for Cbr-Lox mice has been described (6). Mx-Lox mice were typed with PCR primers MXF5 (5' GGTGCTGTGAAGGAGTGGAA 3') and MXR5 (5' GAACAGTAGCCCATCTGCCA 3') for the wild type allele and MXPF2 (5' GGACGGTTGGAGAAGAAGGT 3') and MXPR2 (5' CCACCAAAGAACGGAGCC 3') for the mutant allele. Duplications of the DSCR were typed by PCR primers CBRHF2B (5' CACCTTCTTCTCCAACCGTC 3') and MXPR2, deletions with CBRHR2 (5' CTCGTCCTGCAGTTCATTCA 3') and MXPF2. PCR reactions contained 2 mM MgCl<sub>2</sub> and were performed for 30 cycles of denaturation (30 s 94 °C), annealing (1 min 55 °C), and extension (45 s 72 °C). Mice were maintained in a virus antibody-free colony and given breeder chow and water ad libitum. All procedures were approved by the Institutional Animal Care and Use Committee.

FISH mapping with BACs 401C2 and 433G17 was performed as described (8). BAC 401C2 labeled with Spectrum Green and BAC 433G17 labeled with Spectrum Orange. BAC 401C2 is found outside the targeted region (proximal to *Cbr1*) whereas BAC 433G17 is within the targeted region. Chromosomes were counterstained with DAPI II (Vysis) and viewed with a Zeiss Axioskop using a SenSys CCD camera (Photometrics) and Quips Smart Capture imaging software (Applied Imaging, Santa Clara, CA). 20 interphase cells with two green and red signals were analyzed, producing results like those in Fig. 1e and 1f.

Mice. F1 progeny of the founder chimera were backcrossed to (B6 x C3H) $F_n$  mice to produce Ts1Rhr and euploid mice that inherited 50% of their genetic information from B6, 25% from 129 and 25% from C3H strain mice. Male Ms1Rhr F1 mice were crossed to female Ts65Dn mice to produce Ts65Dn, Ms1R/Ts65Dn and euploid mice with the same genetic background. For morphometric analysis, mice were sacrificed and carcasses were skinned and gutted and put into a Dermestid beetle colony for cleaning. Three-dimensional locations of cranial and mandibular landmarks were recorded directly from the skeletons using the Reflex microscope. Three-dimensional coordinate locations of 11 landmarks located on the left side of the cranium and 7 on the left mandible of Ts65Dn (N=12) and normal littermates (N=23), Ts1Rhr (N=9) and normal littermates (N=8), and Ms1Rhr/Ts65Dn (N=10) and normal littermates (N=6) were recorded directly from the skeletons using the Reflex microscope (9) (Fig. S3).

The observer was blinded to the karyotype of each mouse during data collection. Landmark coordinate data were analyzed using EDMA (10) to provide a statistical test of similarity in craniofacial shape between mouse models for DS and their normal littermates. EDMA is a landmark-based morphometric method that uses consistent estimators of the mean form based on distances between landmarks to determine statistical differences between samples. Importantly, any procedure based on the EDMA parameters is invariant to the choice of the translation matrix and to rotation and reflection (11, 12). EDMA enables testing of a null hypothesis of similarity in shape for portions of the craniofacial skeleton defined by a specific subset of landmarks using a nonparametric bootstrapping procedure (13). Moreover, EDMA enables localization of statistically significant similarities and differences in form through nonparametric bootstrapping procedures that calculate confidence intervals ( $\alpha = 0.10$ ) for all linear distances being compared between segmentally trisomic mice and euploid littermates (14). If this interval contains the value 1.0, the null hypothesis of similarity for that linear distance cannot be rejected. EDMA programs are down loadable from <http://oshima.anthro.psu.edu>. Raw data are available from JTR.

For growth analysis, (B6 x 129)F1 Ms1Rhr and Ts1Rhr mice were weighed beginning at post-natal day 14. Data presented for the first two points were collected  $\pm 2$  days, for the third point  $\pm 4$  days, and for the fourth point  $\pm 7$  days. The number of male plus female animals at each data point varied from 4 to 30. Asterisks indicate significant differences ( $\alpha = 0.05$ ) among the three groups using single factor ANOVA.

Supplemental figures

Figure S1: Phenotype maps of HSA21. The DSCR in Ts1Rhr mice corresponds to region 'B'. The critical region features assigned to subregions of the DSCR (designated A and B) are from Delabar and Korenberg (13, 14). Features marked with an \* have parallels in Ts65Dn mice. Based on Ensembl sequence, *D21S17* is 436 kb proximal to *CBRI* and this interval contains one gene, *C21orf18*. The interval between *MX2* and *BCEI* (the latter is now known as *TFF1*) contains eight genes. *Tff1* is found in the mouse on MMU17.

Fig. S1

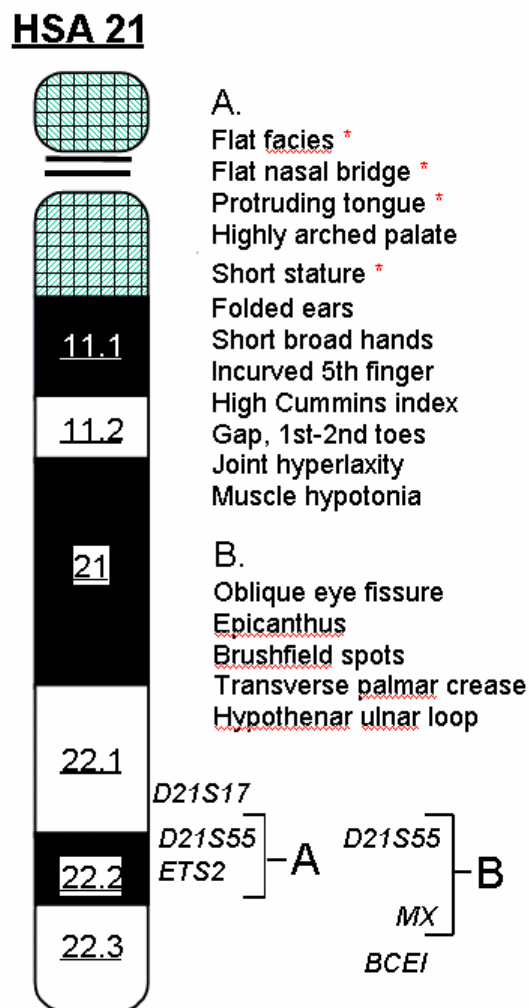


Figure S2: Comparison of regions and number of genes triplicated in the segmental trisomy models of Down syndrome. Sizes in MB refer to the homologous regions of HSA21. The number of genes in each segment is based on the “conserved” plus “minimally conserved” gene categories of Gardiner et al. (15). The red segment is the Down syndrome critical region (DSCR) described by Delabar and colleagues (6). Font colors used for genes listed in Table S1 correspond to green, blue, red and purple segments on this figure.

Fig. S2

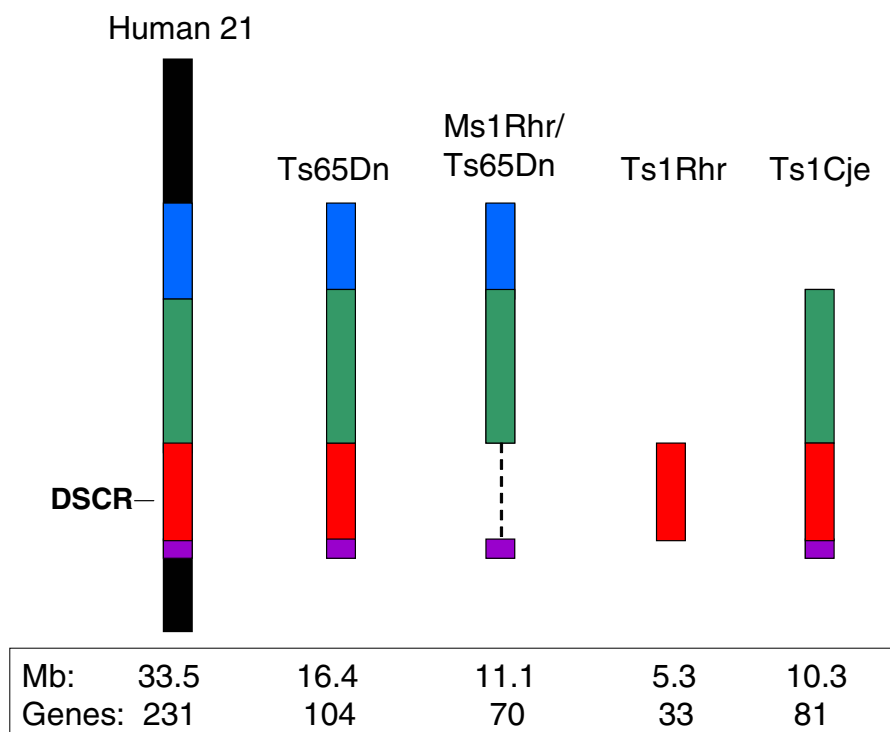


Figure S3. Landmarks located on the left crania and hemi-mandibles of mice used in analysis. Skulls were cleaned by Dermestid beetles and then visualized using the Reflex microscope that enables the recording of 3D landmarks coordinates. Data are checked for measurement error following methods outlined elsewhere (Richtsmeier, *et al.*, 1995). After initial checks for gross measurement error, landmark data are collected twice from immobilized skulls and the coordinate locations of the two trials are averaged to reduce intra-observer error. The average landmark locations are used in EDMA analysis. The landmarks on the crania include: 1, nasale; 2, nasion; 3, bregma; 4, intersection of parietal and interparietal bones; 5, intersection of interparietal and occipital bones at the midline; 6, center of alveolar ridge over maxillary incisor; 7, most inferior point on premaxilla-maxilla suture; 8, anterior notch on frontal process lateral to infraorbital fissure; 9, intersection of frontal process of maxilla with frontal and lacrimal bones; 10, joining of squamosal body to zygomatic process of squamosal; 11, intersection of parietal, temporal and occipital bones. Landmarks on the mandible include: 12, coronoid process; 13, anterior-most point on mandibular condyle; 14, posterior-most point on mandibular condyle; 15, mandibular angle; 16, inferior-most point on border of ramus inferior to incisor alveolar, 17, superior-most point on incisor alveolar rim (at bone-tooth junction); 18, anterior point on molar alveolar rim.

Fig. S3

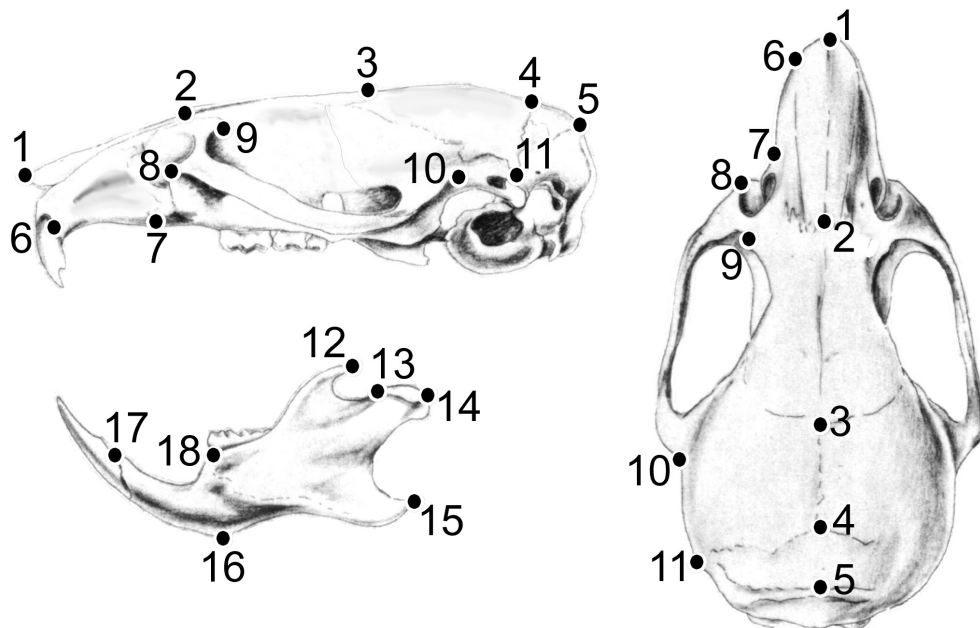


Table S1. Orthologous genes found on HSA21 and MMU16 in various DS mouse models, based on Gardiner et al. (18). Colors correspond to the segments shown in Figure S2.

#	Name	Class	Accession number (human)	Accession number (mouse)	Domain, functional associations and similarities
1	PRED22-MRPL39	C	AK000458	BC016561	Mitochondrial ribosomal protein L39
2	C21orf43-JAM2	C	AY077698	AJ291757	Vascular endothelial junction-associated protein;
3	ATP5A	C	NM_001685	BC010766	immunoglobulin superfamily ATP synthase, H <sup>+</sup> transporting, mitochondrial F0 complex, subunit F6 (ATP5J), nuclear gene encoding mitochondrial protein
4	GABPA	C	U13044	BB843469 BC013562	nuclear respiratory factor-2 subunit alpha; ETS domain transcription factor
5	APP	C	NM_000484	X59379	amyloid beta (A4) precursor protein (protease nexin-II, Alzheimer disease)
6	CYYR1	C	AK054581	AF442733 BF018515	Cysteine, tyrosine-rich
7	ADAMTS1	C	AF207664	D67076	matrix metalloprotease
8	ADAMTS5	C	NM_007038	NM_011782	a disintegrin-like and metalloprotease (reprolysin type) with thrombospondin type 1 motif, 5 (aggrecanase-2)
9	N6AMT1-PRED28	C	NM_013240	AK012019	Putative N6-DNA-methyltransferase
10	ZNF294	C	AB018257 AK001915	BC027795 BB818828 AK019706	Ring-finger domain
11	C21orf6	C	NM_016940	BC002143	Ring-finger domain and WD repeat domain
12	USP16	C	AF126736	AK004594	Ubiquitin processing protease (Ubp-M)
13	CCT8	C	NM_006585	NM_009840	Chaperonin containing TCP1, subunit 8 (theta)
14	C21orf7	C	NM_020152	AY033899 BB63836 BB639676	TAB2 binding domain of TAK1; interleukin 1 signaling pathway ?
15	BACH1	C	AB002803	NM_007520	BTB-basic leucine zipper transcription factor
16	as-BACH1	MC		AW107038 AW011823	
17	GRIK1	C	L19058	X66118	Glutamate receptor (GLUR5)
18	AK016377	C	AK016377	AK016377	
19	CLDN17	C	AJ250712	BB369077 BB648933	Cell adhesion molecule at tight junctions; 4 transmembrane domains
20	CLDN8	C	AJ250711	BC003868	Cell adhesion molecule at tight junctions; 4 transmembrane domains

21	KRTAPcluster	C			
22	TIAM1	C	U16296	NM_009384 BB641865	G-nucleotide exchange factor for Rac
23	SOD1	C	X02317	BC002066	Superoxide dismutase
24	SFRS15	C	AF023142	BC024860 BG964143 BG974812 BG404789 BB646927	Similar to pre-mRNA splicing SR proteins
25	MAK5-HUNK	C	NM_014586	NM_015755	Hormonally upregulated Neu-associated kinase
26	BI731159	MC		BI731159	
27	C21orf45	C	AF231921	AK012533	
28	C21orf61	C	AF454915	AK003912	Transmembrane domain; fat cell-specific low molecular weight protein beta (FALP)
29	C21orf108-KIAA0539	C	AF231919	BF608283 AA670781 BBG14563 BB614563 AV149698 BB438600 AK017495	6 transmembrane domains
30	C21orf63	C	AF358258	BB630672 AK016443	2 SUEL domains (galactose-binding lectin domains)
31	C21orf59	C	AK000474	AK018510	
32	SYNJ1	C	AF009040	AU067566 AU079361 BB327282 AW492248 BE646742 BB645565 AW045957	Phosphoinositol phosphatase
33	GCFC-C21orf66	C	AY033906	AY033908	Spliceosomal-associated
34	C21orf62	C	AF231922	NM_028905 BB862520	Signal sequence
35	Olig2-bHLHoleg2	C	AF221520	BE862632 AB038697	basic helix-loop-helix transcription factor class B 1 (BHLHB1)
36	Olig1-bHLHoleg1	C	BC026989	AB038696	basic helix-loop-helix transcription factor
37	IFNAR2	C	NM_000874	NM_010509	Interferon (alpha, beta and omega) receptor 2
38	IL10RB	C	Z17227	AF440787	Cytokine receptor
39	IFNAR1	C	J03171	NM_010508	Interferon-alpha receptor
40	IFNGR2	C	U05875	NM_008338	Interferon gamma receptor accessory factor-1 (AF-1)
41	C21orf4	C	AF045606	BC004841	4 transmembrane domains
42	as-GART	MC		BB613384	
43	C21orf55	C	AF462153	NM_138664	DnaJ/Hsp40 motif
44	GART	C	X54199	NM_010256	De novo purine biosynthesis
45	SON	C	AF380179	NM_019973	G-patch and ds RNA binding motif
46	C21orf60	C	AF232673	BC018792	

47	CRYZL1	C	NM_005111	AK017995	Crystallin, zeta (quinone reductase)-like 1
48	ITSN	C	AF114487	BB840012 NM_010587	2 EH, 5 SH3, RhoGef, PH, C2 domains
49	ATP5O	C	X83218	NM_138597	ATP synthase oligomycin-sensitivity-conferral subunit
50	MRPS6	C	NM_032476	BC027271	Mitochondrial ribosomal protein S6
51	SLC5A3	C	AF027153	NM_017391	Na-myo-inositol cotransporter
52	KCNE2	C	AF302095	NM_134110	voltage-gated K <sup>+</sup> channel; ISK-related; subunit MIRP1
53	C21orf51	MC	AY081144	NM_138743	
54	AK016199	C	AK016199	AK016199	
55	KCNE1	C	BI459541	AK008938	Voltage-gated K <sup>+</sup> channel, ISK-related
56	BB644499	MC		BB644499	
57	DSCR1	C	NM_004414	AF263240	Inhibitor of Calcineurin
58	AK010774	MC		AK010774	
59	CLIC6	C	BG702259 BF872299 BG184920	BB873551 AI527485 AW990844	Putative Chloride channel
60	uf09c04	MC		AI227398	
61	RUNX1	C	D43969	NM_009821	Runt domain transcription factor; disrupted in Acute Myelogenous Leukemia 1
62	AK007778	C	AK007778	AK007778	
63	BB651311	MC		BB651311	
64	C21orf18	C	AK001660	AY037804	
65	CBR1	C	J04056	NM_007620	Carbonyl reductase
66	CBR3	C	NM_001236	BC028763	Carbonyl reductase
67	C21orf5	C	NM_005128	AK002808 AK012087	
68	AK009785	MC		AK009785	
69	KIAA0136	C	D50926	BB610032 BB819028 BF163187 BC026506	ATP-binding domains
70	CHAF1B	C	BC021218	AK011243	Chromatin assembly factor
71	CLDN14	C	AF314090	AF314089	Cell adhesion protein in tight junctions
72	SIM2	C	U80456	NM_011377	Transcription factor; HLH, 2 PAS, 1 PAC domain
73	HLCS	C	D87328	AB066227 BB659806	Holocarboxylase synthase
74	DSCR6	MC	AB037158	NM_133229	
75	DSCR5	C	AF216305	NM_019543	2 transmembrane domains; Down syndrome critical region protein 5
76	TTC3	C	BG393989 D84294	BB665467 NM_009441	Tetratricopeptide repeats
77	DSCR3	C	D87343	NM_007834	Vacuolar protein sorting-associated protein (Vps) 26 motif
78	DYRK1A	C	AF108830	U58497	serine-threonine protein kinase;



				AK009788	tyrosine phosphorylation regulated
79	as-DYRK1	C	AA729988	AA729988	
80	KCNJ6	C	NM_002240	U51124	Potassium inwardly-rectifying channel, subfamily J, member 6
81	KCNJ15	C	NM_002243	AJ012368	Potassium inwardly-rectifying channel, subfamily J, member 15
82	as-KCNJ15	MC		AK015140	
83	ERG	C	M17254	NM_133659 BB655125	ETS-related; SAM/Pointed and ETS domains; transcription factor
84	ETS2	C	NM_005239	BC005486	v-ets erythroblastosis virus E26 oncogene homolog 2 (avian); transcription factor
85	DSCR2	C	AJ006291	NM_019537	Leucine rich
86	WDR9	C	AJ292465	AJ292467	8 Trp-Aps domains; 2 bromo (DNA binding ) domains
87	HMG14	C	NM_004965	AK010763	high-mobility group (nonhistone chromosomal) protein 14
88	WRB	C	Y12478	AK021091	Signal sequence; 2 transmembrane domains; trp-rich C terminus
89	C21orf13	C	BC031059	BB614664	
90	SH3BGR	C	X93498	AJ272170	Signal sequence; Pro-rich putative SH3 domain; Glu-rich C-terminus
91	B3GALT5	C	AB020337	BI660749 NM_033149	UDP-Gal:betaGlcNAc beta 1,3-galactosyltransferase, polypeptide 5
92	IGSF5	C	BG740428	AK008060	immunoglobulin superfamily, member 5
93	PCP4	C	U52969	BE980230 NM_008791	PEP19; brain specific peptide
94	DSCAM	C	NM_001389	AY005483	Down syndrome cell adhesion molecule
95	as-DSCAM	MC		AK016518	
96	BACE2	C	AF178532	NM_019517	Aspartate protease; b-site APP cleavage
97	MX1	C	M33882	M21038	Interferon-induced cellular resistance mediator protein; Dynamin and Dynamin GTPase effector domains
98	C21orf11	C	AJ409094	AF360358	
99	MX2	C	M30818	AB029920	Interferon-induced cellular resistance mediator protein; Dynamin and Dynamin GTPase effector domains
100	TMPRSS2	C	NM_005656	AF199362	1 transmembrane domain; serine protease
101	ANKRD3	C	NM_020639	AF302127	Kinase domain; 10 ankyrin domains
102	ZNF298-C21orf83	C	AY078498	AY063457	SET domain; 17 zinc finger domains
103	C21orf25	C	AL050173	AF416778 BG243938	C2 calcium binding domain

104 ZNF295 C AB033053 AK017896 BB625951 BTB protein interaction domain;  
8 zinc finger domains

\* Highly conserved (C) = majority of coding exons >70% identity between species. Minimally conserved (MC) = evidence of gene structure (spliced ESTs or consistent exon prediction) present in only one species and/or few exons > 65% identity over > 50 nucleotides.

#### References

1. C. N. Adra, P. H. Boer, M. W. McBurney, *Gene* **60**, 65-74 (1987).
2. J. M. Ahearn, Jr., M. S. Bartolomei, M. L. West, L. J. Cisek, J. L. Corden, *J Biol Chem* **262**, 10695-705 (Aug 5, 1987).
3. R. S. Sikorski, P. Hieter, *Genetics* **122**, 19-27 (May, 1989).
4. T. Yagi *et al.*, *Proc Natl Acad Sci U S A* **87**, 9918-22 (Dec, 1990).
5. M. T. Pletcher, T. Wiltshire, D. E. Cabin, M. Villanueva, R. H. Reeves, *Genomics* **74**, 45-54. (2001).
6. L. E. Olson *et al.*, *Cancer Res* **63**, 6602-6 (Oct 15, 2003).
7. A. Puech *et al.*, *Proc Natl Acad Sci U S A* **97**, 10090-5 (Aug 29, 2000).
8. C. S. Moore *et al.*, *Genomics* **59**, 1-5 (Jul 1, 1999).
9. J. T. Richtsmeier, L. L. Baxter, R. H. Reeves, *Dev Dyn* **217**, 137-45. (2000).
10. S. Lele, J. Richtsmeier, *An invariant approach to the statistical analysis of shapes*, Interdisciplinary studies in statistics. (Chapman and Hall/CRC Press, London, 2001).
11. S. Lele, C. McCulloch, *J Amer Stat Assoc* **971**: 796-806 (2002)
12. J.T. Richtsmeier, V.B. DeLeon, S. Lele *Yrbk of Phys. Anthropol.* **45**:63-91 (2002)
13. S. Lele, J. T. Richtsmeier, *Am J Phys Anthropol* **86**, 415-27. (1991).
14. S. Lele, J. T. Richtsmeier, *Am J Phys Anthropol* **98**, 73-86. (1995).
15. J. M. Delabar *et al.*, *Eur J Hum Genet* **1**, 114-24 (1993).
16. J. R. Korenberg *et al.*, *Proc Natl Acad Sci U S A* **91**, 4997-5001 (1994).
17. J.T. Richtsmeier *et al.*, *Cleft Palate-Craniofacial Journal* **32**: 217-227 (1995).
18. K. Gardiner, A. Fortna, L. Bechtel, M. T. Davisson, *Gene* **318**, 137-47 (2003).